

Siklos, Pierre L.; Stefan, Martin; Wellenreuther, Claudia

Article — Published Version

Metal prices made in China? A network analysis of industrial metal futures

Journal of Futures Markets

Provided in Cooperation with:

John Wiley & Sons

Suggested Citation: Siklos, Pierre L.; Stefan, Martin; Wellenreuther, Claudia (2020) : Metal prices made in China? A network analysis of industrial metal futures, Journal of Futures Markets, ISSN 1096-9934, Wiley, Hoboken, NJ, Vol. 40, Iss. 9, pp. 1354-1374, <https://doi.org/10.1002/fut.22125>

This Version is available at:

<https://hdl.handle.net/10419/230161>

Standard-Nutzungsbedingungen:

Die Dokumente auf EconStor dürfen zu eigenen wissenschaftlichen Zwecken und zum Privatgebrauch gespeichert und kopiert werden.

Sie dürfen die Dokumente nicht für öffentliche oder kommerzielle Zwecke vervielfältigen, öffentlich ausstellen, öffentlich zugänglich machen, vertreiben oder anderweitig nutzen.

Sofern die Verfasser die Dokumente unter Open-Content-Lizenzen (insbesondere CC-Lizenzen) zur Verfügung gestellt haben sollten, gelten abweichend von diesen Nutzungsbedingungen die in der dort genannten Lizenz gewährten Nutzungsrechte.

Terms of use:

Documents in EconStor may be saved and copied for your personal and scholarly purposes.

You are not to copy documents for public or commercial purposes, to exhibit the documents publicly, to make them publicly available on the internet, or to distribute or otherwise use the documents in public.



If the documents have been made available under an Open Content Licence (especially Creative Commons Licences), you may exercise further usage rights as specified in the indicated licence.



<http://creativecommons.org/licenses/by/4.0/>

RESEARCH ARTICLE

Metal prices made in China? A network analysis of industrial metal futures

Pierre L. Siklos¹ | Martin Stefan²  | Claudia Wellenreuther^{2,3} 

¹Department of Economics, Wilfrid Laurier University, Waterloo, Ontario, Canada

²Department of Economics, Westfälische Wilhelms-Universität Münster, Münster, Germany

³Department of Energy and Environmental Economics, Hamburg Institute of International Economics (HWWI), Hamburg, Germany

Correspondence

Martin Stefan, Department of Economics, Westfälische Wilhelms-Universität Münster, Am Stadtgraben 9, 48143 Münster, Germany.
Email: martin.stefan@wiwi.uni-muenster.de

Abstract

In addition to being the world's greatest consumer and producer of industrial metals, China now also features the most actively traded industrial metal futures contracts worldwide. To examine China's role in the global price formation process of industrial metal futures markets, we use a sample of 29 futures contracts traded on exchanges in the United States, the United Kingdom, India, and China. We estimate vector autoregressive models and conduct variance decompositions, which are then visualized in the form of networks. The results indicate that China, despite its role as key actor in both real and financial industrial metal markets, is a price taker.

KEYWORDS

China, commodity markets, industrial metals, networks, price leadership

1 | INTRODUCTION

China's rapid industrialization and rise as an economic power have been accompanied by a voracious appetite for natural resources. This is particularly visible in the country's demand for industrial metals. As the country continues its process of urbanization and investment in infrastructure, China has evolved into the world's top consumer of refined aluminum, copper, nickel, steel, and zinc. In 1980, when China's policy of reform was just beginning, the country's share in worldwide consumption of these metals ranged between 3% and 4%. Today, Chinese consumption makes up 40% of the world's demand for lead and nickel and 50% of the world's demand for aluminum, copper, and zinc (World Bank, 2018). Similarly, the country has also developed into the top producer of these metals. In 2017, roughly half of all steel, refined aluminum and zinc, and 40% of refined copper and lead were produced in China (World Bank, 2018).

Moreover, China's importance in the market for metals is not limited to the real side of the economy. Chinese commodity futures exchanges have, over the years and following a series of regulatory changes, evolved into the world's largest futures markets for numerous industrial metals. As documented by the Futures Industry Association's (FIA) 2018 volume survey, seven out of the ten most traded industrial metal futures contracts are traded on Chinese exchanges (Acworth, 2019). Moreover, the Shanghai Futures Exchange's (SHFE) steel rebar futures contract has grown into the most traded commodity futures contract worldwide.

In light of these developments, this paper investigates the role of Chinese price leadership in industrial metal futures markets. We gather futures price data on 29 industrial metal contracts traded on six exchanges in the United States, the United Kingdom, India, and China. Our study is the most comprehensive analysis of industrial metal futures conducted to date. It includes futures contracts for copper, lead, nickel, iron, and several kinds of steel, and thus covers a much

This is an open access article under the terms of the Creative Commons Attribution License, which permits use, distribution and reproduction in any medium, provided the original work is properly cited.

© 2020 The Authors. *The Journal of Futures Markets* published by Wiley Periodicals LLC

larger variety of commodities than earlier studies. To answer the question of whether China has become a price leader in these markets, the network approach of Diebold and Yilmaz (2012, 2014) is used, which rests on variance decompositions of vector autoregressive (VAR) models' forecast errors. Based on these decompositions, so-called connectedness tables are compiled which summarize how shocks to a specific futures price travel through the system of all prices of this commodity. These connectedness tables are then visualized in the form of graphical networks. Finally, we explore, via regressions, whether we can identify some economic and financial determinants of connectedness.

We obtain two main findings. Chinese metal contracts are strongly interconnected with contracts traded on other exchanges. Thus, there are significant information flows between Chinese and selected Western exchanges. However, in these relationships, China is typically a net receiver of price shocks and not a large sender. Instead, price discovery is roughly equally shared between the U.S.-American, British, and Indian futures markets. This implies that China, despite its role as leading consumer, producer, and trader of industrial metals, is a price taker in the corresponding futures markets. Consequently, other factors hinder Chinese exchanges from playing a more important role in the global price formation process. A key factor in this regard might be the investor structure of Chinese commodity futures exchanges, which differs from its Western counterparts. First, government regulation largely excludes foreign investors from participating in Chinese markets. Second, various news accounts document that Chinese metal futures are traded by a large number of uninformed retail investors (see e.g., Financial Times, 2016a, 2016b).

The remainder of this paper is structured as follows. Section 2 summarizes important steps in the development of Chinese commodity futures markets and earlier research on their role as price leader. Thereafter, Section 3 explains the data used in this paper, while Section 4 introduces the methodology. Section 5 then presents the key results, and Section 6 analyzes the determinants of connectedness. Section 7 concludes.

2 | INSTITUTIONAL BACKGROUND AND RELATED LITERATURE

Today, Chinese futures trading occurs on five futures exchanges. The Dalian Commodity Exchange (DCE) and the Zhengzhou Commodity Exchange (ZCE) mainly focus on agricultural and chemical products, while the SHFE covers various metal contracts. Financial and crude oil futures contracts are traded at the China Financial Futures Exchange (CFX) and the Shanghai International Energy Exchange (INE).

Despite the fact that Chinese futures markets continue to be relatively closed to foreign investors, who must generally rely on domestic intermediaries to conduct trades on their behalf,¹ many Chinese futures contracts now outstrip their Western counterparts in terms of trading volume. In international comparisons, Chinese metal futures contracts trade in remarkably high trading volumes, which is not surprising given the stylized facts outlined in the introduction. According to the FIA 2018 volume survey, seven out of the ten most traded industrial metal futures contracts are all traded on Chinese exchanges (Acworth, 2019). Moreover, the SHFE steel rebar futures contract has grown into the most traded commodity futures contract in the world.

Against this backdrop, and given the fact that China has, over the years, evolved into the largest consumer and producer of numerous industrial metals (World Bank, 2018), a sizable body of literature has investigated the role of Chinese futures exchanges as potential price leaders in industrial metals. Being among the oldest industrial metal futures contracts traded in China, the SHFE's copper contract has been analyzed in numerous studies. Fung, Leung, and Xu (2003) use data from 1995 to 2001 and conduct a bivariate GARCH analysis of two copper futures contracts traded at the SHFE and the New York Commodity Exchange (COMEX). They find that the American contract dominates the information flow between the two markets. Liu and An (2011) study the same contracts but make use of a VECM-GARCH framework and a price discovery metric developed by Lien and Shrestha (2009). The authors use data from 2004 to 2009 and conclude that the U.S. market generally leads its Chinese counterpart and is also dominant in the price discovery process. Li and Zhang (2013) study the case of copper on a broader basis by considering, in addition to the contracts traded at the SHFE and the COMEX, the contracts traded at the London Metal Exchange (LME) and the Multi Commodity Exchange (MCX) in Mumbai, India. Employing an SVAR model and data ranging from 2005 to 2011, the authors' results suggest that the LME contract is the key price maker. Conversely, the results of Rutledge, Karim,

¹Exceptions pertain to the INE's crude oil contract, the DCE's iron ore contract and the ZCE's Purified Terephthalic Acid (PTA) contract, which, following a new directive by the China Securities Regulatory Commission (2015), can be traded directly by qualified foreign brokerage firms without the need for a domestic intermediary.

and Wang (2013), who use a VECM estimation and Granger-causality tests based on data from 2006 to 2011, reveal no distinct leadership pattern between the copper contracts traded at the SHFE, LME, and COMEX.

Studies featuring multiple metal contracts include that of Hua and Chen (2007), who study the markets for copper and aluminum. Using data from 1998 to 2002, the authors consider contracts traded at the SHFE and the LME. They employ Granger-causality tests and find that the LME contracts Granger-cause those of the SHFE, which implies that the Chinese contracts are price followers. Fung, Liu, and Tse (2010), who consider aluminum and copper contracts traded at the SHFE and the COMEX, use data from 1999 to 2009 and employ a VECM which accounts for structural breaks. They find that neither market dominates the information flow between them. Fung, Tse, Yau, and Zhao (2013) investigate the case of Chinese price leadership on an even broader basis by considering 16 different commodities including aluminum, copper, and zinc contracts traded at the SHFE and the LME. The authors' data range from different starting dates for each contract until 2011 and are analyzed using various regression techniques including error correction and GARCH models. Again, no clear pattern is found, as mixed and bidirectional results are obtained for the different industrial metal contracts. Lastly, the study by Kang and Yoon (2016), which is closely related to our work, uses the approach proposed by Diebold and Yilmaz (2012) to study the SHFE's and LME's futures contracts for aluminum, copper, and zinc. Using data from 2007 to 2016, the authors find that price shocks typically originate in the LME's contracts and then travel to those of the SHFE.²

The present paper extends this earlier research in three important ways: First, by analyzing 29 different contracts, some of which were launched as recently as November 2015, it is the most comprehensive study of industrial metal futures conducted to date. As our analysis covers futures contracts for copper, lead, nickel, iron, and several kinds of steel, we investigate a much larger variety of commodities than earlier studies. Second, by conducting variance decompositions of the forecast errors of various systems of different futures contracts, the network approach of Diebold and Yilmaz (2012, 2014) enables us to graphically visualize the inter-dependencies between the different contracts. Third, we go beyond reporting market connectedness to consider the potential economic determinants of this phenomenon.

3 | DATA

To examine the role of Chinese price leadership in the market for industrial metal futures, we gather data on 29 industrial metal contracts at daily frequency beginning in November 2004 until August 2019. All price time series are retrieved from Thomson Reuters Datastream, whereby continuous series are constructed by switching to the nearest contract on the first day of each new trading month. The sample ranges for the individual commodity groups are dictated by the availability of data for the youngest futures contract in that group. Table 1 lists the contracts used in the analysis and details the different contract specifications such as notation and size.

Our sample covers five aluminum contracts, one cobalt contract, four copper contracts, one ferrosilicon contract, two iron ore contracts, three lead and nickel contracts, one silicon manganese contract, five steel contracts, one tin contract and three zinc contracts. The contracts are traded on six different exchanges, namely the COMEX, the LME, the MCX (in Mumbai, India), the SHFE, the DCE, and the ZCE.³

Figure 1 displays the futures price time series of the commodity contracts included in our analysis. All prices have been converted to USD per metric ton (USD/mt). In accordance with the law of one price, we observe relatively similar price movements among the different contracts for each type of commodity. Nonetheless, Chinese prices are most of the time noticeably higher for all commodities. This could be due to barriers to trade concerning the Chinese market. Regarding the steel market, we observe the greatest price differences within one commodity. This is because of the different types of steel included in our sample, which range from steel rebar to steel coils and steel scrap. The same holds for the aluminum market, where one can see large price differences between the LME's aluminum alloy contract and the other pure aluminum contracts. The unusual behaviour of the COMEX's aluminum price starting in late 2017 can be explained by the exceptionally low trading volumes of this contract.

Summary statistics of the daily logarithmic futures returns are displayed in Table 2. The daily returns range from -0.32% to 0.33% . Standard deviations range from 0.01 to 0.02. Roughly two-thirds of all return series exhibit a negative skewness, suggesting that severe price drops are more common than large price increases. For all return series we

²Other applications of variance decompositions or the network approach of Diebold and Yilmaz (2012) to the case of Chinese commodity markets, include the studies of Yang and Leatham (1999) and Zhang and Wang (2014) who consider the markets for wheat and crude oil.

³Note that the COMEX is since 2008 owned by the CME Group, while the LME is since 2012 owned by Hong Kong Exchanges and Clearing.

TABLE 1 Industrial metal futures contracts

| Contract | Exchange | Notation | Size |
|-------------------|----------|----------|-----------|
| Aluminum | COMEX | USD/mt | 25 mt |
| Aluminum | LME | USD/mt | 25 mt |
| Aluminum Alloy | LME | USD/mt | 20 mt |
| Aluminum | MCX | INR/kg | 5 mt |
| Aluminum | SHFE | RMB/mt | 5 mt |
| Cobalt | LME | USD/mt | 1 mt |
| Copper | COMEX | USD/lbs | 25,000 lb |
| Copper | LME | USD/mt | 25 mt |
| Copper | MCX | INR/kg | 1 mt |
| Copper | SHFE | RMB/mt | 5 mt |
| Ferrosilicon | ZCE | RMB/mt | 5 mt |
| Iron Ore | DCE | RMB/mt | 100 mt |
| Iron Ore | COMEX | USD/mt | 500 mt |
| Lead | LME | USD/mt | 25 mt |
| Lead | MCX | INR/kg | 5 mt |
| Lead | SHFE | RMB/mt | 5 mt |
| Nickel | LME | USD/mt | 6 mt |
| Nickel | MCX | INR/kg | 250 kg |
| Nickel | SHFE | RMB/mt | 1 mt |
| Silicon Manganese | ZCE | RMB/mt | 5 mt |
| Steel Scrap | LME | USD/mt | 10 mt |
| Steel Rebar | LME | USD/mt | 10 mt |
| Steel Coils | COMEX | USD/st | 20 st |
| Steel Rebar | SHFE | RMB/mt | 10 mt |
| Steel Coils | SHFE | RMB/mt | 10 mt |
| Tin | LME | USD/mt | 5 mt |
| Zinc | LME | USD/mt | 25 mt |
| Zinc | MCX | INR/kg | 5 mt |
| Zinc | SHFE | RMB/mt | 5 mt |

Note: Contract sizes are reported in “mt,” “kg,” “st,” and “lb” referring to metric tons, kilograms, short tons (equivalent to roughly 0.907 metric tons), and pounds (equivalent to 0.453 kilograms), respectively.

Abbreviations: COMEX, New York Commodity Exchange; DCE, Dalian Commodity Exchange; INR, Indian rupee; LME, London Metal Exchange; MCX, Multi Commodity Exchange (Mumbai, India); RMB, Chinese renminbi; SHFE, Shanghai Futures Exchange; USD, U.S. dollar; ZCE, Zhengzhou Commodity Exchange.

observe kurtosis values well in excess of 3, which is the reference kurtosis value of the normal distribution. This implies that none of the series follow a normal distribution but feature fat tails instead.

4 | METHODOLOGY

To investigate the price leadership in the metal futures market, we follow the financial market connectedness approach of Diebold and Yilmaz (2012, 2014). Within this framework, the informational spillovers between different metal

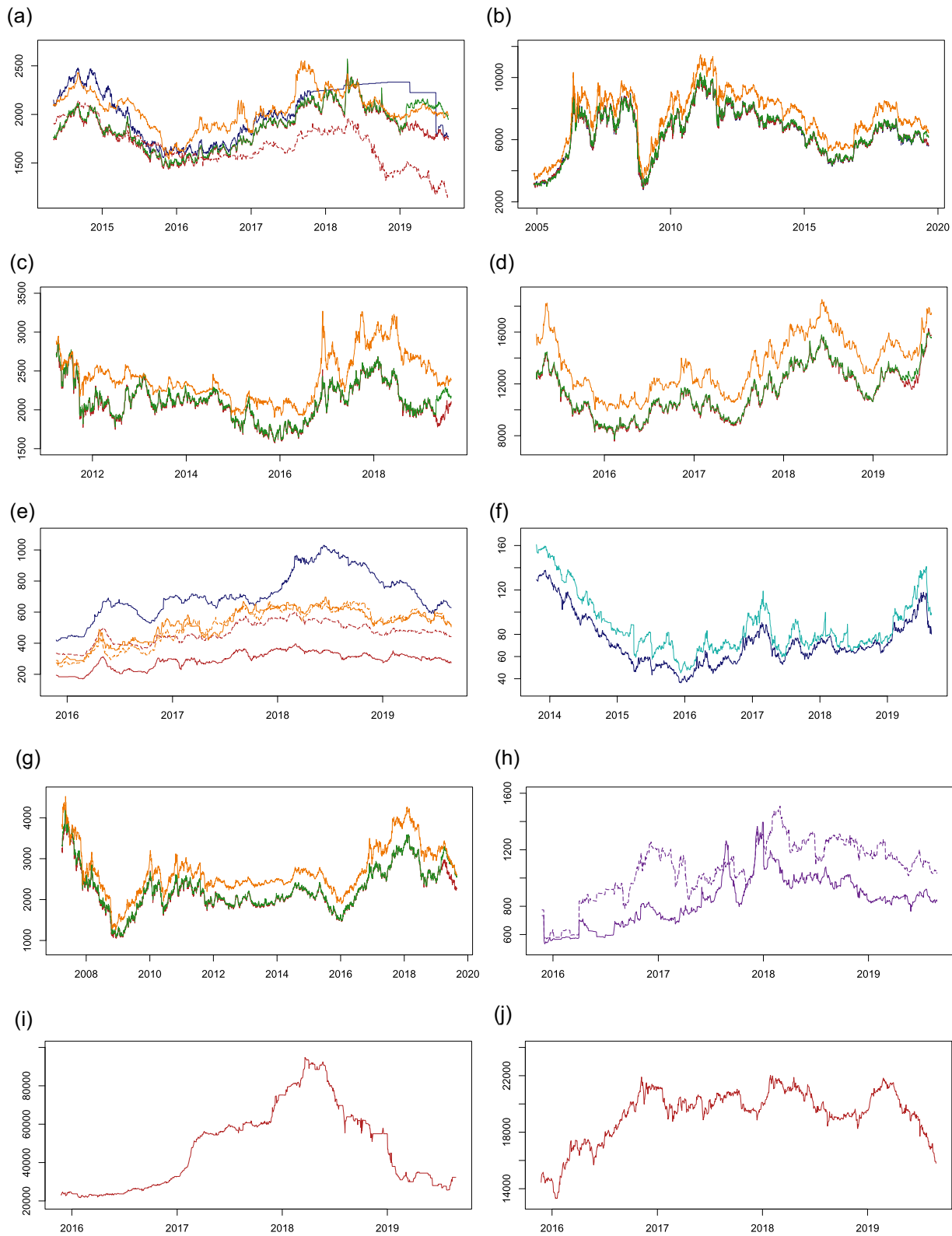


FIGURE 1 Futures price time series. COMEX contracts are highlighted in blue, LME contracts in red, MCX contracts in green, SHFE contracts in orange, DCE contracts in cyan, ZCE contracts in purple. Steel rebar, aluminum alloy, and the silicon manganese contracts are depicted using dashed lines. All prices have been converted to USD/mt. Subfigures (a) through (j) show the price time series for aluminum, copper, lead, nickel, steel, iron, zinc, silicons, cobalt and tin, respectively [Color figure can be viewed at wileyonlinelibrary.com]

TABLE 2 Summary statistics of returns

| Contract | Exchange | Obs. | Min | Mean | Max | SD | Skew. | Kurt. |
|-------------------|----------|-------|-------|-------|------|------|-------|--------|
| Aluminum | COMEX | 1,385 | -0.20 | -0.00 | 0.04 | 0.01 | -6.22 | 130.07 |
| Aluminum | LME | 1,386 | -0.08 | -0.00 | 0.05 | 0.01 | 0.18 | 5.91 |
| Aluminum Alloy | LME | 1,386 | -0.07 | -0.00 | 0.06 | 0.01 | -0.24 | 9.39 |
| Aluminum | MCX | 1,386 | -0.10 | 0.00 | 0.08 | 0.01 | 0.39 | 11.13 |
| Aluminum | SHFE | 1,386 | -0.04 | -0.00 | 0.04 | 0.01 | 0.19 | 5.86 |
| Cobalt | LME | 982 | -0.16 | 0.00 | 0.12 | 0.02 | -0.58 | 18.76 |
| Copper | COMEX | 3,854 | -0.12 | 0.00 | 0.12 | 0.02 | -0.13 | 7.19 |
| Copper | LME | 3,854 | -0.10 | 0.00 | 0.12 | 0.02 | -0.01 | 7.51 |
| Copper | MCX | 3,853 | -0.12 | 0.00 | 0.10 | 0.02 | -0.10 | 7.68 |
| Copper | SHFE | 3,854 | -0.07 | 0.00 | 0.06 | 0.01 | -0.28 | 6.27 |
| Ferrosilicon | ZCE | 982 | -0.28 | 0.00 | 0.20 | 0.02 | -2.70 | 55.71 |
| Iron Ore | DCE | 1,527 | -0.32 | -0.00 | 0.10 | 0.02 | -2.91 | 32.73 |
| Iron Ore | COMEX | 1,528 | -0.09 | -0.00 | 0.16 | 0.02 | 0.15 | 6.93 |
| Lead | LME | 2,199 | -0.08 | -0.00 | 0.08 | 0.02 | -0.01 | 5.17 |
| Lead | MCX | 2,199 | -0.09 | -0.00 | 0.09 | 0.01 | 0.11 | 6.38 |
| Lead | SHFE | 2,198 | -0.05 | -0.00 | 0.05 | 0.01 | -0.17 | 7.59 |
| Nickel | LME | 1,153 | -0.09 | 0.00 | 0.07 | 0.02 | -0.18 | 4.64 |
| Nickel | MCX | 1,153 | -0.08 | 0.00 | 0.07 | 0.02 | -0.01 | 4.52 |
| Nickel | SHFE | 1,152 | -0.06 | 0.00 | 0.06 | 0.01 | -0.08 | 5.29 |
| Silicon Manganese | ZCE | 982 | -0.28 | 0.00 | 0.33 | 0.02 | 0.42 | 68.77 |
| Steel Scrap | LME | 981 | -0.08 | 0.00 | 0.10 | 0.02 | -0.22 | 7.06 |
| Steel Rebar | LME | 981 | -0.05 | 0.00 | 0.05 | 0.01 | 0.05 | 6.01 |
| Steel Coils | COMEX | 982 | -0.06 | 0.00 | 0.11 | 0.01 | 1.65 | 18.87 |
| Steel Rebar | SHFE | 982 | -0.09 | 0.00 | 0.10 | 0.02 | -0.18 | 7.80 |
| Steel Coils | SHFE | 982 | -0.08 | 0.00 | 0.08 | 0.02 | 0.10 | 7.59 |
| Tin | LME | 982 | -0.07 | 0.00 | 0.04 | 0.01 | -0.35 | 6.09 |
| Zinc | LME | 3,242 | -0.11 | -0.00 | 0.10 | 0.02 | -0.05 | 5.43 |
| Zinc | MCX | 3,242 | -0.09 | -0.00 | 0.10 | 0.02 | -0.07 | 5.68 |
| Zinc | SHFE | 3,242 | -0.06 | -0.00 | 0.05 | 0.01 | -0.39 | 5.71 |

Abbreviations: COMEX, New York Commodity Exchange; DCE, Dalian Commodity Exchange; LME, London Metal Exchange; MCX, Multi Commodity Exchange (Mumbai, India); SHFE, Shanghai Futures Exchange; ZCE, Zhengzhou Commodity Exchange.

futures contracts are studied using a network interpretation of a VAR model's variance decomposition. The starting point of this approach is estimating the following covariance stationary VAR(p) model:

$$\mathbf{r}_t = \sum_{i=1}^p \Phi_i \mathbf{r}_{t-i} + \boldsymbol{\varepsilon}_t, \quad (1)$$

where the vector $\mathbf{r}_t = (r_{1,t}, r_{2,t}, \dots, r_{n,t})'$ contains n logarithmic futures return time series, and $\boldsymbol{\varepsilon}_t$ is an $n \times 1$ vector of white noise disturbances with covariance matrix $\boldsymbol{\Omega}$.⁴

⁴As our empirical application includes 29 futures return time series, we use an elastic net shrinkage approach based on Zou and Hastie (2005) to eliminate statistically superfluous variables and improve the performance of the VAR.

4.1 | Forecast error variance decomposition

The VAR model above can be represented as a vector moving average (VMA) model of the form

$$\mathbf{r}_t = \sum_{i=0}^{\infty} \Psi_i \varepsilon_{t-i}, \quad (2)$$

where Ψ_i denotes the $n \times n$ moving average coefficient matrices. These are determined by $\Psi_i = \Phi_1 \Psi_{i-1} + \Phi_2 \Psi_{i-2} + \dots + \Phi_p \Psi_{i-p}$ for $i > 0$, while $\Psi_0 = \mathbf{I}_n$ and $\Psi_i = \mathbf{0}$ if $i < 0$. Based on the VMA model in Equation (2), one can compute the generalized H -step ahead forecast error variance decompositions d_{ij}^H of Koop, Pesaran, and Potter (1996) and Pesaran and Shin (1998) as

$$d_{ij}^H = \frac{\sigma_{jj}^{-1} \sum_{h=0}^{H-1} (\mathbf{e}_i' \Psi_h \Omega \mathbf{e}_j)^2}{\sum_{h=0}^{H-1} (\mathbf{e}_i' \Psi_h \Omega \Phi_h' \mathbf{e}_i)}, \quad (3)$$

where σ_{jj} is the standard deviation of $\varepsilon_{j,t}$, while \mathbf{e}_i is the $n \times 1$ selection vector consisting of zeros only except for its i -th element, which is equal to one. This decomposition captures the contribution that shocks to variable j make to the H -step-ahead error variance when forecasting variable i . In the case of $i = j$, Diebold and Yilmaz (2012) refer to d_{ij}^H as the *own variance share*. Correspondingly, if $i \neq j$, d_{ij}^H is called the *cross variance share*.

Note that this type of variance decomposition, unlike conventional variance decompositions, does not make use of a Cholesky factorization of Ω and is thus independent of the ordering of the time series in the system. However, as the shocks to the model's variables are not orthogonalized, a variable i 's different variance shares due to shocks in variable j generally do not add up to one, that is $\sum_{j=1}^n d_{ij}^H \neq 1$. Therefore, to allow straightforward comparisons between the different shocks sent by a variable j to another variable i , the variance decompositions are normalized and converted into percentages by computing

$$\tilde{d}_{ij}^H = \frac{d_{ij}^H}{\sum_{j=1}^n d_{ij}^H} \cdot 100. \quad (4)$$

Thus, by construction, $\sum_{j=1}^n \tilde{d}_{ij} = 100$ and $\sum_{i,j=1}^n \tilde{d}_{ij} = n \cdot 100$.⁵

4.2 | Measuring connectedness

Following Diebold and Yilmaz (2014), the variance decomposition computed above can be interpreted as a measure of the H -step ahead *gross* pairwise directional connectedness from variable j to variable i , that is

$$C_{i \leftarrow j}^H = \tilde{d}_{ij}^H. \quad (5)$$

As $C_{i \leftarrow j}^H$ will generally not be equal to $C_{j \leftarrow i}^H$, the net flow of shocks between the two variables, or *net* pairwise directional connectedness from variable j to variable i , is calculated as

$$C_{ij}^H = \tilde{d}_{ji}^H - \tilde{d}_{ij}^H. \quad (6)$$

To gauge a variable's relative importance as sender or receiver of shocks in the system, Diebold and Yilmaz (2014) compute two measures of *total* directional connectedness. The first of these measures, $C_{i \leftarrow \cdot}^H$, summarizes all those parts of a variable i 's forecast error variance decomposition that are due to shocks *from* another variable j . Hence, this measure is calculated as

$$C_{i \leftarrow \cdot}^H = \sum_{\substack{j=1, \\ j \neq i}}^n \tilde{d}_{ij}^H. \quad (7)$$

⁵An alternative forecast error variance decomposition is developed by Lanne and Nyberg (2016).

Conversely, the second measure $C_{i \leftarrow j}^H$ summarizes all the contributions that variable i makes to the forecast error variance of another variable j . This measure is therefore given by

$$C_{i \leftarrow j}^H = \sum_{\substack{i=1, \\ i \neq j}}^n \tilde{d}_{ij}^H. \tag{8}$$

The difference between these two metrics is the *net* total directional spillover

$$C_{i \leftrightarrow \cdot}^H = C_{i \leftarrow \cdot}^H - C_{\cdot \leftarrow i}^H. \tag{9}$$

If a market's net spillover is above zero, the market sends more shocks than it receives. Conversely, if the market's net spillover is below zero, the market is a net receiver of price signals.

Lastly, to capture the system's total connectedness, Diebold and Yilmaz (2014) sum up all of the normalized cross variance shares. To allow for comparing the total connectedness values of different variable systems, this measure C^H is also normalized by n :

$$C^H = \frac{1}{n} \sum_{\substack{i,j=1, \\ i \neq j}}^n \tilde{d}_{ij}^H. \tag{10}$$

It holds by construction that the system's total connectedness is equal to the (normalized) sum of all shocks sent or equivalently all shocks received.

Given these measures of connectedness, a *connectedness table* for the VAR system of Equation (1) is constructed as follows: Table 3.

The main diagonal elements, apart from C^H , display how the variance of a specific return series is driven by the series's own shocks. The off-diagonal elements, except those at the margin of the connectedness table, represent the fraction of a return series's variance that is due to shocks in the other return series. The bottom row elements summarize the total impact that the return series have on the variance of the other return series, while the elements of the right-most column summarize the total of shocks that the return series receive from the other series in the system. Thus, the greater a futures return series' total directional connectedness, the greater its role in price leadership. Conversely, if a return series features a large row sum, it features a high total directional connectedness from others and is therefore a strong recipient of price signals originating from other futures contracts.

Our analysis covers 29 different futures price time series, rendering an analysis of all impulse response functions unfeasible. However, as shown by Diebold and Yilmaz (2014), the variance decompositions matrix described above can be interpreted as a network. The nodes of this network are the different variables of the VAR system, that is, in our case the different metal futures contracts, while the connections between the contracts are determined by the magnitudes of the different variance decompositions. The advantage of interpreting the variance decompositions in this way is that it allows for straightforward visualizations of market interdependencies and information flows using previously developed graph-drawing algorithms, which are discussed below in greater detail.

TABLE 3 Concept of connectedness tables

| | r_1 | r_2 | ... | r_n | From others |
|-----------|----------------------------|----------------------------|-----|----------------------------|----------------------------|
| r_1 | $C_{1 \leftarrow 1}^H$ | $C_{1 \leftarrow 2}^H$ | ... | $C_{1 \leftarrow n}^H$ | $C_{1 \leftarrow \cdot}^H$ |
| r_2 | $C_{2 \leftarrow 1}^H$ | $C_{2 \leftarrow 2}^H$ | ... | $C_{2 \leftarrow n}^H$ | $C_{2 \leftarrow \cdot}^H$ |
| ⋮ | ⋮ | ⋮ | ⋮ | ⋮ | ⋮ |
| r_n | $C_{n \leftarrow 1}^H$ | $C_{n \leftarrow 2}^H$ | ... | $C_{n \leftarrow n}^H$ | $C_{n \leftarrow \cdot}^H$ |
| To others | $C_{\cdot \leftarrow 1}^H$ | $C_{\cdot \leftarrow 2}^H$ | ... | $C_{\cdot \leftarrow n}^H$ | C^H |

Note: Connectedness table as proposed by Diebold and Yilmaz (2014).

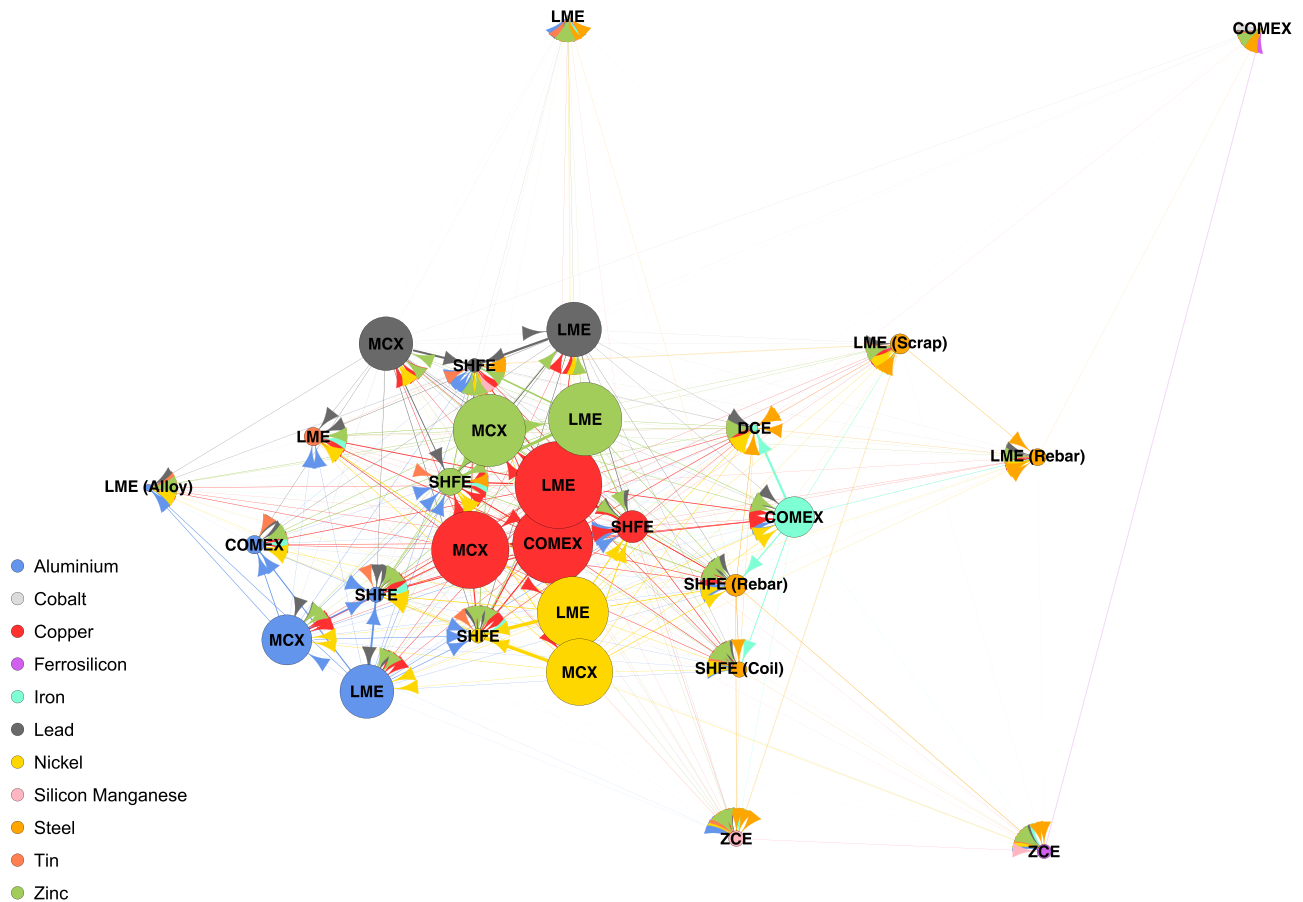


FIGURE 2 Network representation of return spillovers. Node size depends on total directional spillovers, arrow thickness and direction on net pairwise directional spillovers. Node placement is based on the graph-drawing algorithm of Fruchterman and Reingold (1991). COMEX, New York Commodity Exchange; DCE, Dalian Commodity Exchange; LME, London Metal Exchange; MCX, Multi Commodity Exchange; SHFE, Shanghai Futures Exchange; ZCE, Zhengzhou Commodity Exchange [Color figure can be viewed at wileyonlinelibrary.com]

5 | VISUALIZING THE METAL NETWORK

We first consider the entire sample of industrial metal futures contracts explained in the data section. The resulting system comprises 29 contracts across 11 different commodities traded on six futures exchanges in four countries. The sample size is thereby limited by the contracts with the most recent starting dates. These are the SHFE's steel contracts, which started trading in November 2015. The sample ends in August 2019. We implement the variance decomposition procedure described above⁶ and, following Diebold and Yilmaz (2014), we interpret the resulting connectedness table as a network. As explained before, each node in the network resembles one of the futures contracts.

Figure 2 visualizes this network based on the graph-drawing algorithm developed by Fruchterman and Reingold (1991). This algorithm draws networks by balancing attracting and repelling forces between its nodes. In our network two nodes attract each other depending on their pairwise directional spillovers C_{ij}^h . The net pairwise directional spillovers, that is, the differences between the two shocks flowing between two contracts, are shown as arrows between the nodes. They point in the direction of the larger shock between the two contracts and are thicker the greater the net directional spillover. The nodes repel each other depending on their size, which is determined by the total directional connectedness to others $C_{\leftarrow j}^H$. Consequently, strong net senders of shocks will feature large nodes with numerous

⁶Based on the Schwarz-Bayes information criterion, we selected one lag for the VAR model and, following Diebold and Yilmaz (2012), we chose a forecast horizon of $H = 10$ days. In a robustness exercise we altered this forecast horizon to 5 and 20 days, respectively, but did not obtain any significantly different results. The results of this robustness exercise are available upon request.

arrows pointing away from them. Conversely, strong recipients have smaller nodes and many arrows pointing toward them. Lastly, the nodes are highlighted in different colors depending on the contracts' underlying commodities.

The network visualization reveals distinct clusters of contracts based on the underlying commodity groups to which they belong. Copper contracts are located close to other copper contracts, aluminum contracts close to other aluminum contracts, and so on. Only the steel contracts (highlighted in orange) are relatively spread out, but they still form a cluster. The steel cluster partly surrounds the iron cluster (highlighted in cyan) reflecting the close relationship between the two commodities, as iron is the key input factor in the steel production. This finding echoes the results of Indriawan, Liu, and Tse (2019) who analyzed the market quality and connectedness of Chinese metal futures and found that iron ore and steel rebar contracts are highly connected with another.

The center of the network is dominated by the different copper contracts (highlighted in red). Apart from their placement in the center of the network, the nodes of these contracts are also considerably larger than those of other commodity groups, underscoring their importance for the network. Similar results have been obtained in other network analyses of copper spot and futures prices. For example, Wang, Zhang, Li, Chen, and Wei (2019), Xiao, Yu, Fang, and Ding (2019), and Guhathakurta, Dash, and Maitra (2020) show that copper is highly interconnected with other commodities and an important transmitter of price and volatility shocks. This is in line with the fact that copper is one of the most widely used industrial metals, featuring applications in construction, electrical and electronic products, transportation and consumer products. Therefore, copper is often seen as an indicator for the state of the overall economy. Moreover, Indriawan et al. (2019) show that, at least for the case of Chinese metal futures markets, copper futures exhibit the greatest level of market quality in terms of low bid-ask spreads, low pricing error, and a high probability of informed trading.

The nickel and zinc clusters (highlighted in green and yellow, respectively) also feature relatively large nodes that are also placed toward the center of the network. This reflects their great importance in the real metal market, where nickel and zinc are highly connected to other metals, as they are used for the galvanization and production of stainless steel and other ferro-alloys. The aluminum and lead clusters (highlighted in blue and gray, respectively) tend toward the periphery of the network but are not as distant from the center as the contracts for cobalt, ferrosilicon, silicon manganese, and tin. In the network, lead is closely connected to zinc, reflecting the fact that lead is a common byproduct in the zinc mining process.

Concerning the Chinese futures contracts, we find that these contracts are, despite their large trading volumes, generally of minor importance to the network, as indicated by their relatively small node sizes and the high number of arrows pointing toward them. Conversely, Western and Indian markets are of greater importance. Interestingly, we find no strong difference between Western and Indian markets in their ability to contribute to the price discovery process as indicated by the same size of their nodes in the network. For example, concerning the copper contracts, we find that the total directional spillovers originating from the COMEX, the LME and the MCX toward other exchanges amount to 129.67, 140.58, and 125.10, respectively, while the spillovers of the SHFE amount to only 51.91.⁷

Possible reasons for this are the fact that Chinese financial markets, as documented by Liu, Tse, and Zhang (2018), remain relatively closed to foreign investors. In addition, the same authors also detail that Chinese markets are heavily driven by financial speculation and retail investors instead of large institutional investors. Consequently, Chinese markets might not utilize new information about market fundamentals as efficiently as their Western and Indian counterparts. Compared to one another, these markets are approximately of equal importance in the global price formation process.

In a second step, we now consider the financial connectedness within the different clusters of commodities observed above. In this regard, we examine six clusters, namely those of aluminum, copper, lead, nickel, zinc, and the combined cluster of iron and steel. As before, the sample sizes are limited by the youngest contract in each cluster.⁸ The resulting subnetworks are shown in Figure 3. The subnetworks confirm the earlier impression that Chinese market participants are price takers. In all of the six clusters, the Chinese contracts feature the smallest nodes. Despite their placement, often in the center of the networks, they are major recipients of shocks from the others markets, as shown by the net pairwise directional spillovers pointing toward them.

⁷Similar results are obtained for the nickel (zinc) contracts, where the total directional spillovers from the LME and the MCX toward other exchanges amount to 115.07 (118.55), 107.71 (117.01), while the SHFE's spillover only amounts to 23.27 (43.90). The full connectedness Table A1, which is the basis for the network depicted in Figure 2, is provided in the appendix.

⁸The aluminum sample starts on May 6, 2014, the copper sample on November 18, 2004, the lead sample on March 24, 2011, the nickel sample on March 27, 2015, the iron and steel sample on November 23, 2015, and the zinc sample on March 26, 2007. All samples end on August 27, 2019.

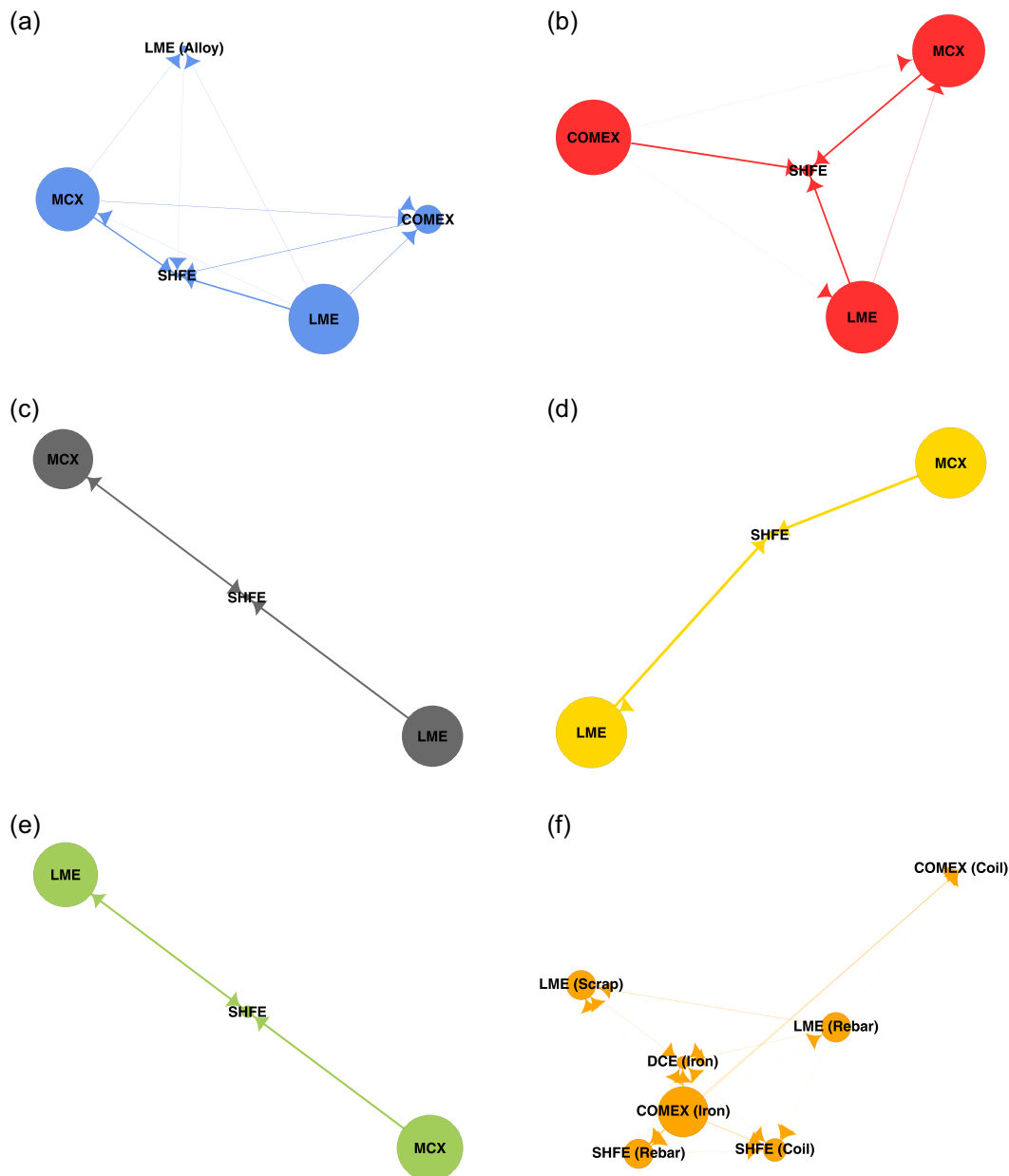


FIGURE 3 Individual commodity networks. Node size depends on total directional spillovers, arrow thickness, and direction on net pairwise directional spillovers. Node placement is based on the graph-drawing algorithm of Fruchterman and Reingold (1991). COMEX, New York Commodity Exchange; DCE, Dalian Commodity Exchange; LME, London Metal Exchange; MCX, Multi Commodity Exchange; SHFE, Shanghai Futures Exchange; ZCE, Zhengzhou Commodity Exchange [Color figure can be viewed at wileyonlinelibrary.com]

To study the subnetworks over time, we employ rolling window estimations of the underlying VAR models with a window size of 250 trading days, which is equal to one trading year. In each step, we follow the variance decomposition procedure as before. Thereafter, we advance the window by 1 day for the subsequent estimation. Consequently, we obtain for each day and futures contract the total directional spillovers *to others* and *from others*. While the former spillover indicator measures the amount of shocks sent by the different markets, the latter captures the amount of shocks received by each of them. As explained earlier, computing the differences between these two metrics yields the *net* total directional spillovers (see Equation (9)). Figure 4 displays these time-varying *net* total directional spillovers of each futures contract.

The graphs show that for most of the commodity clusters, the net spillovers range between -60 and 30 . However, the steel market exhibits far smaller net spillovers ranging from only -20 to 10 . This suggests that the iron and steel market is less integrated than the other commodity groups, which is not surprising given the varied composition of

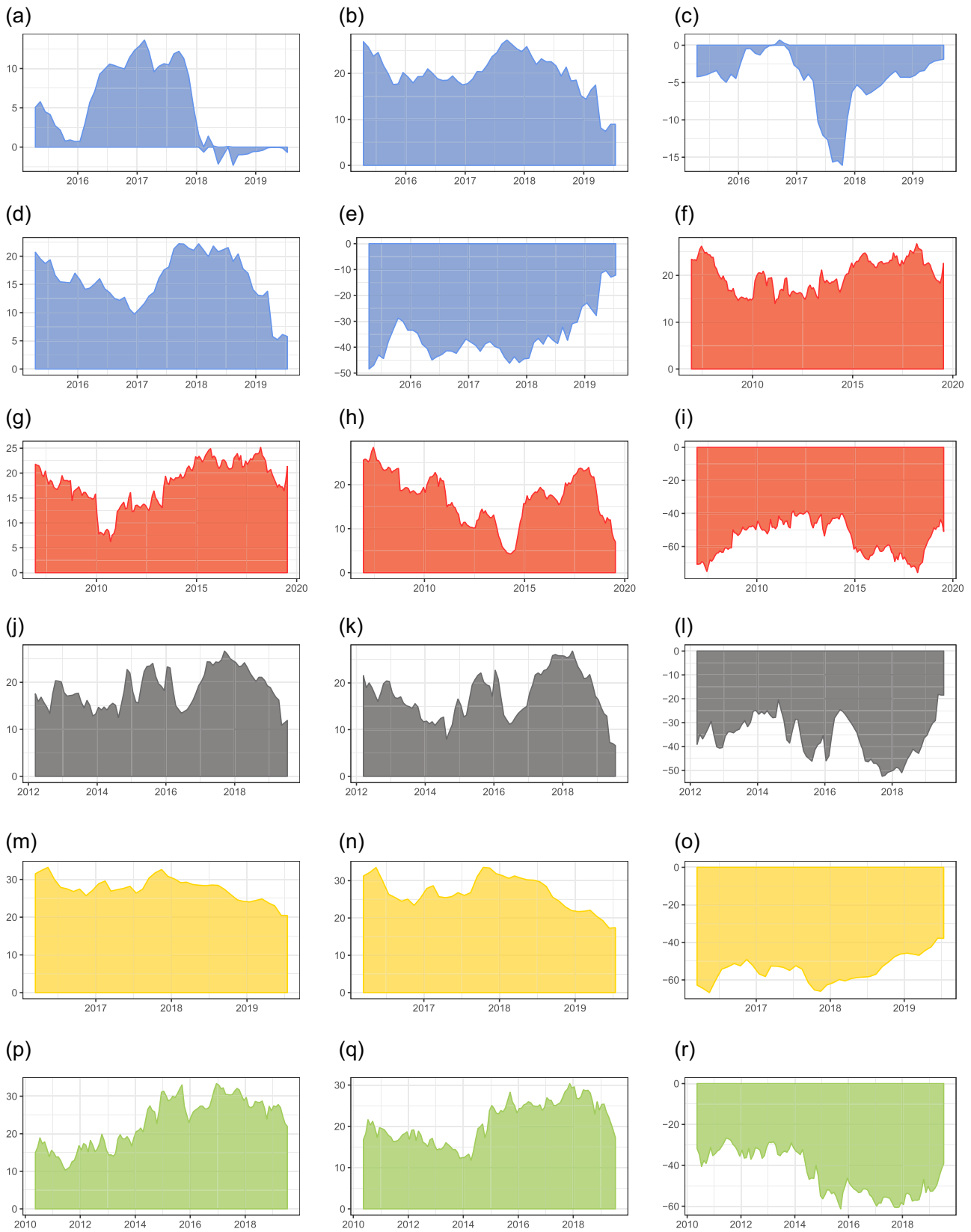


FIGURE 4 Time-varying net spillovers. The graphs show monthly averages of the time-varying net total directional spillovers of each futures contract. Values above zero indicate that a contract sends more price signals than it receives, whereas values below zero suggest the opposite [Color figure can be viewed at wileyonlinelibrary.com]

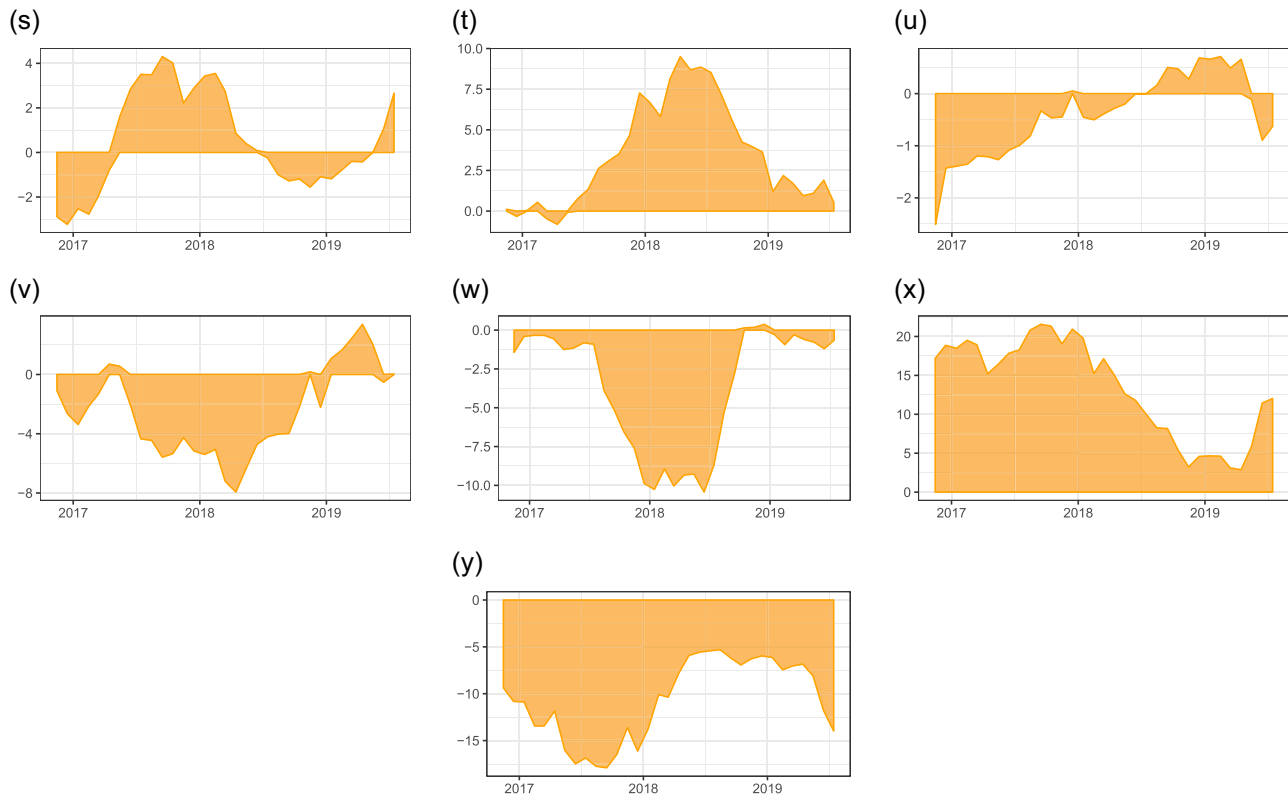


FIGURE 4 (Continued)

these contracts (rebar, coils, etc.). This corresponds to what was shown in Figure 2, where the steel and iron contracts were relatively spread out. The net spillovers of Chinese contracts are almost always below zero and relatively stable over time, consistent with our earlier finding that the Chinese exchanges are net receivers of shocks.

One concern with these result is the issue of nonsynchronous trading, as our analysis features futures contracts traded in four different time zones, each 3 to 5 hr apart from the next. A practical solution to this problem is the use of lower frequency data such as weekly or even monthly data. However, this solution is not feasible as many of the contracts in our analysis are relatively young. Hence, there are insufficient observations available to properly estimate the VAR model, even when using weekly data. Also, the equations of the VAR model include the lags of all other prices in the system which controls for previous price movements at the other exchanges.⁹

6 | DETERMINANTS OF CONNECTEDNESS

In this section, we analyze which factors determine if a market is a sender or a receiver of price signals. To do so, we regress the pairwise directional spillovers $C_{i \leftarrow j, t}^{10}$ (see Equation (5)) between contracts j and i on several exogenous variables. In particular we estimate for each of the commodity subnetworks the following dynamic panel fixed effects regression:

$$\begin{aligned}
 C_{i \leftarrow j, t}^{10} = & \beta_0 + \beta_1 C_{i \leftarrow j, t-1}^{10} + \beta_2 VOLA_{j, t} + \beta_3 ILLIQ_{j, t} \\
 & + \beta_4 SPMAT_{j, t} + \beta_5 IM_{ij, t} + \beta_6 EX_{ij, t} \\
 & + \beta_7 TED_{j, t} + \beta_8 VIX_{j, t} + \beta_9 EPU_{j, t} + \varepsilon_{j, t}.
 \end{aligned} \tag{11}$$

⁹Alternatively, one might consider the use of intra-day data and an event study approach. However, reliance on this kind of data raises other challenges that are beyond the scope of this paper.

Apart from the lagged spillover variable $C_{i \leftarrow j, t-1}^{10}$, we consider three groups of exogenous variables, namely financial variables, variables related to real economic activity and variables measuring credit risk and market uncertainty. The financial group includes the variables $VOLA_{j,t}$ and $ILLIQ_{j,t}$. $VOLA_{j,t}$ refers to the relative market volatility of contract j , which is based on the conditional volatility estimates of an AR(1)-GARCH(1,1) model of contract j 's returns. $ILLIQ_{j,t}$ is a proxy for market illiquidity proposed by Amihud (2002), which relates the absolute value of a market's return to its trading volume. High values of this ratio indicate illiquid market environments, whereas low values of this measure suggest high levels of liquidity. It is generally expected that liquidity increases a market's ability to process new information.

The second group of variables, which capture economic activity, comprise the regressors $SPMAT_{j,t}$, $IM_{ij,t}$, and $EX_{ij,t}$. To control for regional supply and demand shocks, we consider the S&P 500 Materials $SPMAT_{j,t}$ for the United States, Europe, India, and China. $IM_{ij,t}$ and $EX_{ij,t}$ refer to the imports and exports flowing between country i and country j , whereby $IM_{ij,t}$ represents the amount of the underlying commodity that country j imports from i , while $EX_{ij,t}$ denotes exports from j to i . Another important economic variable is the exchange rate. We consider the dollar exchange rate of the currency the contract is denominated in. If a contract is denominated in dollars, which is the case for contracts traded at the COMEX and the LME, we use the inverse of the trade-weighted U.S. dollar index, called the broad index.

However, given the interdependencies between exports, imports and the exchange rate and the resulting endogeneity problem, we do not add the exchange rate in the main regression. Instead we follow an instrumental variables approach using a two-stage least square estimation. In the first stage we regress imports and exports on the lagged values of imports, exports, and the exchange rate. The fitted values of this first stage regression are then used to estimate Equation (11).

The third group comprises the variables $TED_{j,t}$, $VIX_{j,t}$, and $EPU_{j,t}$. The TED-spread $TED_{j,t}$ is a measure for credit risk and is calculated as the difference between the benchmark interbank lending rates and the interest rates of the corresponding government securities. The volatility index $VIX_{j,t}$ captures the volatility of the countries' major stock exchange indices and is a common proxy for market uncertainty. The variable $EPU_{j,t}$ is an index measuring the economic policy uncertainty of the country in which contract j is traded. Lastly, β_0 denotes a constant and $\varepsilon_{j,t}$ the error term.

We obtain data from three sources. Price and volume data are taken from Thomson Reuters Datastream to compute $VOLA_{j,t}$ and $ILLIQ_{j,t}$. Similarly, interest rate data for the $TED_{j,t}$ as well as the $VIX_{j,t}$, and data for the $SPMAT_{j,t}$ and the exchange rates are all retrieved from Thomson Reuters Datastream. Lastly, the economic policy uncertainty indices $EPU_{j,t}$ are developed by Baker, Bloom, and Davis (2016)¹⁰, while $IM_{ij,t}$ and $EX_{ij,t}$ are obtained from the International Trade Centre (ITC).

The results of the regressions are presented in Table 4. The lagged spillovers are significantly positive in all subnetworks indicating that there is persistence in spillover effects. The relative volatility has a significantly negative impact for copper and lead. This indicates that in these commodity groups, contracts with higher volatility send less information to other contracts than contracts with lower levels of volatility. The Amihud-ratio, which captures market illiquidity, is associated with a significantly negative sign in the lead market, which implies that liquidity improves this market's ability to transmit information. Concerning the other real-economy variables, we find that imports and exports show significantly positive influences in the iron and steel and the zinc markets. This suggests that in these subnetworks, real-economy flows drive informational spillovers between the different markets. The impact of the S&P 500 Materials index is significantly positive in the iron and steel network. The results regarding the VIX indices suggest that its impact is market-specific with different signs obtained for the different subnetworks. The EPU indices exhibit a significantly positive influence in the copper and iron and steel networks consistent with the notion that rising policy uncertainty raises spillovers. This is likely also a reflection of how greater uncertainty enhances market interconnectedness. As noted earlier, the markets investigated here are truly global in nature. Finally, the TED-spread is never statistically significant. Nonetheless, many of the estimated coefficients are small and are not as economically significant as, say, own lags though it must be remembered that the data are daily. For example, a one point increase in economic policy uncertainty, raises the pairwise directional spillover in copper by only 0.001 index points, while own connectedness is raised by almost 1 index point.

¹⁰Data for the economic policy uncertainty indices by Baker et al. (2016) are available at <http://www.PolicyUncertainty.com>

TABLE 4 Regression results

| | Aluminum | Copper | Lead | Iron & steel | Zinc |
|--------------------------------|---------------------|----------------------|----------------------|---------------------|---------------------|
| $C_{i \leftarrow j, t-1}^{10}$ | 1.007*** (0.013) | 0.952*** (0.013) | 0.919*** (0.016) | 0.927*** (0.011) | 0.931*** (0.016) |
| $VOLA_{j,t}$ | 0.007 (0.009) | -0.032*** (0.007) | -0.023*** (0.005) | 0.013* (0.007) | -0.027 (0.015) |
| $ILLIQ_{j,t}$ | 0.006 (0.006) | -1.033 (0.881) | -1.034*** (0.160) | 0.000 (0.000) | -9.420 (8.013) |
| $SPMAT_{j,t}$ | -0.000 (0.000) | -0.000 (0.000) | -0.000 (0.000) | 0.001** (0.000) | -0.000 (0.000) |
| $IM_{ij,t}$ | -0.008 (0.007) | 0.000 (0.001) | 0.012 (0.022) | 0.016** (0.008) | 0.013*** (0.002) |
| $EX_{ij,t}$ | -0.009 (0.011) | 0.000 (0.001) | 0.104 (0.188) | 0.004*** (0.001) | 0.014*** (0.002) |
| $TED_{j,t}$ | 0.152 (0.177) | 0.038 (0.024) | -0.097 (0.076) | 0.270 (0.171) | -0.084 (0.046) |
| $VIX_{j,t}$ | -0.008 (0.014) | -0.006 (0.005) | -0.041** (0.011) | -0.000 (0.009) | 0.018** (0.006) |
| $EPU_{j,t}$ | -0.000 (0.000) | 0.001** (0.000) | 0.000 (0.000) | 0.001** (0.000) | 0.000 (0.000) |
| Const. | 0.804 (0.763) | 1.956*** (0.544) | 3.778*** (0.517) | -1.214** (0.504) | 2.713** (1.049) |
| \bar{R}^2 | 0.943 | 0.920 | 0.876 | 0.873 | 0.905 |

Note: The table displays the results of the two-stage panel fixed effects regressions for the different commodity subnetworks. The aluminum sample starts on May 6, 2014, the copper sample on November 18, 2004, the lead sample on March 24, 2011, the nickel sample on March 27, 2015, the iron and steel sample on November 23, 2015, and the zinc sample on March 26, 2007. All samples end on August 27, 2019. Standard errors are displayed in parentheses.

* $p < .1$.

** $p < .05$.

*** $p < .01$.

7 | CONCLUSION

Over the past two decades, China has become the greatest consumer and producer of numerous industrial metals. Moreover, China has recently launched a number of futures contracts for these metals, and these have become some of the most highly traded futures contracts worldwide. This paper investigates the question of whether these new markets are important in the formation of international metal prices. We follow the network approach by Diebold and Yilmaz (2012, 2014) and consider 29 metal contracts, traded on six exchanges in the United States, the United Kingdom, India, and China. Despite their large trading volumes, our results indicate that the Chinese futures contracts are not price leaders.

Our analysis comprised three steps. First, we analyzed the overall network structure across all industrial metal futures contracts included in our sample. Unsurprisingly, futures contracts of the same underlying commodities were grouped closely together. Of these clusters, the copper and zinc clusters were found to be the most important ones regarding the transmission of price signals. Furthermore, the Chinese contracts appeared to play a minor role within the different commodity clusters. In a second step, we repeated the earlier analysis, but for each of the different commodity clusters separately. The results of this step confirm those of the first one: Chinese contracts were again found to be net recipients of price shocks. Next, we conducted time-varying network analyses to study how China's role of price leadership varies over time. The results suggest that China's passive role in the price discovery process is relatively stable over time. Lastly, we used a dynamic fixed effects panel regression to study the determinants of connectedness. Apart from lagged spillovers, relative volatility and real sector flows are the strongest determinants of connectedness.

In conclusion, our results provide strong evidence that metal prices are currently not made in China. Price leadership, however, does not appear to be limited to Western markets, as India also appears to be an important transmitter of price signals. Over the past years, Chinese regulators have been able to develop active futures markets for many different commodities including various industrial metals. However, further steps have to be taken to strengthen the role of Chinese markets in terms of price leadership. Most importantly, Chinese markets must become more accessible to foreign investors. But unless such measures are extended to additional markets, price differentials between Chinese and Western markets will continue to exist, since no arbitrage trading will be possible between these two trading venues. A first step in this direction might be the opening of the DCE iron ore futures contract to overseas investors in May 2018. This will allow foreign investors to provide additional liquidity and exploit price differentials between Western and Chinese futures markets.

Moreover, Chinese regulators should aim for greater participation of institutional investors to dampen the effects of retail investors and noise traders. This will improve the ability of Chinese markets to more accurately pick up new fundamental information and become an important price maker in industrial metals. Finally, it is also likely that, as markets in China mature while opening up to foreign investors, the performance of Chinese markets will change. Together with the impending slowdown of China's economy, there is greater scope for a shift away from behavior associated with price taking.

Future research, using event studies or structural break tests, may reveal whether this policy change alters the importance of this contract in the global price formation process of iron ore.¹¹ Moreover, if Chinese market regulators become more transparent and provide greater information about the investor structure in Chinese commodity futures markets, future work will also be able to examine the role of Chinese retail investors and their impact on Chinese price leadership. Such an extension will also provide useful insights to policy makers and regulators.

ACKNOWLEDGMENTS

We thank the editor Robert Webb and an anonymous referee for helpful comments. We would also like to thank our colleague Christoph Sulewski for his valuable help concerning the network analysis.

DATA AVAILABILITY STATEMENT

The futures price data used in this study are available from Thomson Reuters Datastream (2019). Restrictions apply to the availability of these data, which were used under license for this study. Import and export data used in this study are available from the International Trade Center (2019; <https://marketanalysis.intracen.org/en/home>). Economic policy uncertainty (EPU) data were taken from Baker et al. (2016; <https://www.policyuncertainty.com/>).

ORCID

Martin Stefan  <http://orcid.org/0000-0002-0106-436X>

Claudia Wellenreuther  <http://orcid.org/0000-0001-7329-8221>

REFERENCES

- Acworth, W. (2019). 2018 annual volume survey. *Market Voice*, 5(1). Retrieved from <https://www.fia.org/articles/fia-releases-half-year-data-futures-and-options-volume-trends>
- Amihud, Y. (2002). Illiquidity and stock returns: Cross-section and time-series effects. *Journal of Financial Markets*, 5(1), 31–56.
- Baker, S. R., Bloom, N., & Davis, S. J. (2016). Measuring economic policy uncertainty. *The Quarterly Journal of Economics*, 131(4), 1593–1636. Retrieved from <https://www.policyuncertainty.com/>
- China Securities Regulatory Commission (2015). Interim measures for overseas traders and overseas brokers to manage futures of certain types of futures. Retrieved from <http://www.dce.com.cn/dalianshangpin/fg/fz/jysgzghz/2048658/index.html>
- Diebold, F. X., & Yilmaz, K. (2012). Better to give than to receive: Predictive directional measurement of volatility spillovers. *International Journal of Forecasting*, 28(1), 57–66.
- Diebold, F. X., & Yilmaz, K. (2014). On the network topology of variance decompositions: Measuring the connectedness of financial firms. *Journal of Econometrics*, 182(1), 119–134.

¹¹As previously discussed, our results reveal that both Western and Indian futures exchanges are of greater importance than their Chinese counterparts. Historically, India's commodity futures markets have also been relatively closed to foreign investors. Nevertheless, Chinese price leadership might be impaired by additional factors that do not impede Indian markets. These obstacles include, for example, less weight on the rule of law in China than in India (as measured, e.g., by the World Bank's 2020 governance indicators) and China's relatively heavier state-control of its economy. However, the approach adopted in this paper is unable to identify the relative importance of these institutional factors.

- Financial Times (2016a). China warns off commodities market punters. Retrieved from <https://www.ft.com/content/5094d2e8-1387-11e6-91da-096d89bd2173>
- Financial Times (2016b). Chinese retail investors throw global commodities into a tailspin. Retrieved from <https://www.ft.com/content/be92835e-0dcd-11e6-b41f-0beb7e589515>
- Fruchterman, T. M. J., & Reingold, E. M. (1991). Graph drawing by force-directed placement. *Software: Practice and Experience*, 21(11), 1129–1164.
- Fung, H.-G., Leung, W. K., & Xu, X. E. (2003). Information flows between the U.S. and China commodity futures trading. *Review of Quantitative Finance and Accounting*, 21(3), 267–285.
- Fung, H.-G., Liu, Q. W., & Tse, Y. (2010). The information flow and market efficiency between the U.S. and Chinese aluminum and copper futures markets. *Journal of Futures Markets*, 30(12), 1192–1209.
- Fung, H.-G., Tse, Y., Yau, J., & Zhao, L. (2013). A leader of the world commodity futures markets in the making? The case of China's commodity futures. *International Review of Financial Analysis*, 27, 103–114.
- Guhathakurta, K., Dash, S. R., & Maitra, D. (2020). Period specific volatility spillover based connectedness between oil and other commodity prices and their portfolio implications. *Energy Economics*, 85, 104566.
- Hua, R., & Chen, B. (2007). International linkages of the Chinese futures markets. *Applied Financial Economics*, 17(16), 1275–1287.
- Indriawan, I., Liu, Q., & Tse, Y. (2019). Market quality and the connectedness of steel rebar and other industrial metal futures in china. *Journal of Futures Markets*, 39(11), 1383–1393.
- International Trade Center (ITC) (2019). Market analysis tools portal. Retrieved from <https://marketanalysis.intracen.org/en/home>
- Kang, S. H., & Yoon, S.-M. (2016). Dynamic spillovers between Shanghai and London nonferrous metal futures markets. *Finance Research Letters*, 19, 181–188.
- Koop, G., Pesaran, M., & Potter, S. M. (1996). Impulse response analysis in nonlinear multivariate models. *Journal of Econometrics*, 74(1), 119–147.
- Lanne, M., & Nyberg, H. (2016). Generalized forecast error variance decomposition for linear and nonlinear multivariate models. *Oxford Bulletin of Economics and Statistics*, 78(4), 595–603.
- Li, Z., & Zhang, L. H. (2013). An empirical study of international linkages of the Shanghai copper futures market. *The Chinese Economy*, 46(3), 61–74.
- Lien, D., & Shrestha, K. (2009). A new information share measure. *Journal of Futures Markets*, 29(4), 377–395.
- Liu, Q., & An, Y. (2011). Information transmission in informationally linked markets: Evidence from US and Chinese commodity futures markets. *Journal of International Money and Finance*, 30(5), 778–795.
- Liu, Q., Tse, Y., & Zhang, L. (2018). Including commodity futures in asset allocation in China. *Quantitative Finance*, 18(9), 1487–1499.
- Pesaran, H. H., & Shin, Y. (1998). Generalized impulse response analysis in linear multivariate models. *Economics Letters*, 58(1), 17–29.
- Rutledge, R. W., Karim, K., & Wang, R. (2013). International copper futures market price linkage and information transmission: Empirical evidence from the primary world copper markets. *Journal of International Business Research*, 12(1), 113–131.
- Thomson Reuters Datastream (2019). Refinitiv. Retrieved from <https://www.refinitiv.com/en>
- Wang, Y., Zhang, Z., Li, X., Chen, X., & Wei, Y. (2019). Dynamic return connectedness across global commodity futures markets: Evidence from time and frequency domains. *Physica A: Statistical Mechanics and its Applications*, 123464. Retrieved from <https://www.sciencedirect.com/science/article/pii/S0378437119319326?via%3Dihub>
- World Bank. (2018). Commodity markets outlook, April 2018, World Bank, Washington, DC.
- World Bank (2020). Worldwide governance indicators. Retrieved from <https://info.worldbank.org/governance/wgi/>
- Xiao, B., Yu, H., Fang, L., & Ding, S. (2019). Estimating the connectedness of commodity futures using a network approach. *Journal of Futures Markets*, 40(4), 598–616.
- Yang, J., & Leatham, D. J. (1999). Price discovery in wheat futures markets. *Journal of Agricultural and Applied Economics*, 31(2), 359–370.
- Zhang, B., & Wang, P. (2014). Return and volatility spillovers between China and world oil markets. *Economic Modelling*, 42, 413–420.
- Zou, H., & Hastie, T. (2005). Regularization and variable selection via the elastic net. *Journal of the Royal Statistical Society: Series B (Statistical Methodology)*, 67(2), 301–320.

How to cite this article: Siklos PL, Stefan M, Wellenreuther C. Metal prices made in China? A network analysis of industrial metal futures. *J Futures Markets*. 2020;40:1354–1374. <https://doi.org/10.1002/fut.22125>

APPENDIX A

This appendix shows the connectedness table for the entire network of industrial metal markets considered in this article. The following numbers are used to refer to the different futures markets:

1. Aluminum–COMEX
2. Aluminum–LME

3. Aluminum Alloy LME
4. Aluminum-MCX
5. Aluminum-SHFE
6. Cobalt-LME
7. Copper-COMEX
8. Copper-LME
9. Copper-MCX
10. Copper-SHFE
11. Ferrosilicon-ZCE
12. Iron Ore-DCE
13. Iron Ore-COMEX
14. Lead-LME
15. Lead-MCX
16. Lead-SHFE
17. Nickel-LME
18. Nickel-MCX
19. Nickel-SHFE
20. Silicon Manganese-ZCE
21. Steel Scrap-LME
22. Steel Rebar-LME
23. Steel Coils-COMEX
24. Steel Rebar-SHFE
25. Steel Coils-SHFE
26. Tin-LME
27. Zinc-LME
28. Zinc-MCX
29. Zinc-SHFE

TABLE A1 Connectedness table

| | (1) | (2) | (3) | (4) | (5) | (6) | (7) | (8) | (9) | (10) | (11) | (12) | (13) | (14) | (15) |
|------|-------|-------|-------|-------|-------|-------|-------|-------|-------|-------|-------|-------|-------|-------|-------|
| (1) | 53.62 | 9.75 | 0.46 | 7.26 | 1.25 | 0.08 | 2.70 | 3.67 | 2.50 | 0.29 | 0.13 | 0.03 | 0.77 | 2.01 | 2.09 |
| (2) | 5.44 | 29.91 | 1.39 | 22.12 | 1.14 | 0.00 | 4.22 | 5.17 | 4.46 | 0.42 | 0.00 | 0.01 | 0.75 | 2.68 | 2.77 |
| (3) | 0.63 | 3.49 | 75.07 | 3.70 | 0.68 | 0.17 | 1.33 | 1.56 | 2.23 | 0.72 | 0.02 | 0.14 | 0.77 | 1.05 | 1.40 |
| (4) | 4.15 | 22.64 | 1.51 | 30.62 | 0.97 | 0.01 | 3.48 | 3.85 | 5.65 | 0.41 | 0.01 | 0.07 | 0.65 | 1.79 | 3.72 |
| (5) | 2.32 | 8.53 | 0.73 | 7.03 | 34.08 | 0.07 | 3.65 | 3.89 | 3.29 | 7.01 | 0.03 | 0.12 | 1.47 | 1.72 | 1.56 |
| (6) | 0.14 | 0.00 | 0.21 | 0.05 | 0.19 | 94.45 | 0.03 | 0.43 | 0.06 | 0.27 | 0.12 | 0.07 | 0.20 | 0.55 | 0.17 |
| (7) | 1.03 | 2.88 | 0.36 | 2.32 | 0.84 | 0.00 | 20.42 | 16.72 | 15.35 | 1.88 | 0.00 | 0.01 | 1.94 | 4.57 | 3.63 |
| (8) | 1.33 | 3.35 | 0.41 | 2.44 | 0.77 | 0.08 | 15.87 | 19.39 | 13.63 | 2.05 | 0.00 | 0.06 | 1.78 | 5.12 | 3.70 |
| (9) | 0.97 | 3.10 | 0.62 | 3.82 | 0.64 | 0.01 | 15.58 | 14.58 | 20.73 | 1.71 | 0.03 | 0.01 | 1.56 | 3.35 | 4.92 |
| (10) | 0.82 | 2.21 | 0.39 | 1.83 | 3.11 | 0.06 | 12.16 | 12.53 | 10.51 | 14.32 | 0.05 | 0.21 | 2.05 | 3.46 | 2.81 |
| (11) | 0.23 | 0.07 | 0.02 | 0.07 | 0.09 | 0.09 | 0.05 | 0.05 | 0.15 | 0.28 | 72.37 | 0.34 | 0.68 | 0.05 | 0.05 |
| (12) | 0.26 | 0.53 | 0.23 | 0.57 | 0.42 | 0.06 | 1.82 | 1.94 | 1.52 | 1.50 | 0.34 | 59.34 | 12.14 | 0.76 | 0.59 |
| (13) | 0.65 | 1.22 | 0.43 | 1.01 | 0.88 | 0.08 | 4.67 | 4.71 | 3.80 | 2.80 | 0.38 | 3.48 | 40.58 | 1.59 | 1.22 |
| (14) | 1.06 | 2.53 | 0.40 | 1.66 | 0.44 | 0.14 | 6.33 | 7.46 | 4.57 | 1.03 | 0.01 | 0.07 | 0.91 | 28.20 | 18.01 |
| (15) | 1.09 | 2.61 | 0.52 | 3.43 | 0.29 | 0.04 | 4.97 | 5.34 | 6.65 | 0.75 | 0.01 | 0.04 | 0.68 | 17.85 | 27.95 |
| (16) | 0.67 | 1.47 | 0.21 | 1.25 | 1.72 | 0.17 | 3.76 | 4.73 | 3.65 | 4.51 | 0.04 | 0.13 | 1.22 | 10.22 | 9.05 |
| (17) | 0.98 | 4.04 | 0.25 | 3.20 | 0.93 | 0.00 | 7.22 | 7.98 | 6.47 | 0.95 | 0.00 | 0.00 | 1.65 | 3.46 | 2.86 |
| (18) | 0.86 | 3.71 | 0.33 | 4.74 | 0.80 | 0.00 | 6.61 | 6.65 | 7.95 | 0.82 | 0.01 | 0.01 | 1.50 | 2.24 | 3.73 |
| (19) | 0.73 | 2.70 | 0.32 | 2.48 | 1.99 | 0.00 | 5.19 | 5.58 | 5.02 | 5.73 | 0.00 | 0.14 | 1.51 | 2.12 | 2.11 |
| (20) | 0.05 | 0.23 | 0.10 | 0.41 | 0.21 | 0.11 | 0.36 | 0.41 | 0.57 | 0.81 | 17.52 | 0.55 | 1.15 | 0.51 | 0.40 |
| (21) | 0.14 | 0.37 | 0.17 | 0.39 | 0.40 | 0.15 | 0.93 | 1.06 | 0.94 | 0.85 | 0.76 | 0.26 | 4.41 | 0.37 | 0.22 |
| (22) | 0.04 | 0.12 | 0.08 | 0.32 | 0.12 | 0.10 | 0.72 | 0.55 | 0.79 | 0.25 | 0.32 | 0.39 | 4.18 | 0.22 | 0.27 |
| (23) | 0.03 | 0.01 | 0.10 | 0.02 | 0.01 | 0.19 | 0.08 | 0.02 | 0.01 | 0.20 | 0.09 | 0.00 | 0.21 | 0.06 | 0.26 |
| (24) | 0.49 | 0.89 | 0.19 | 0.85 | 0.89 | 0.30 | 2.33 | 2.66 | 2.11 | 3.85 | 1.76 | 2.57 | 9.05 | 1.24 | 0.95 |
| (25) | 0.45 | 0.93 | 0.08 | 0.61 | 1.72 | 0.09 | 2.40 | 2.39 | 1.92 | 3.33 | 1.34 | 1.05 | 7.17 | 0.96 | 0.78 |
| (26) | 1.21 | 1.95 | 0.28 | 1.46 | 1.28 | 0.07 | 4.58 | 5.37 | 3.88 | 2.13 | 0.06 | 0.25 | 1.86 | 2.87 | 1.82 |

TABLE A1 (Continued)

| | (1) | (2) | (3) | (4) | (5) | (6) | (7) | (8) | (9) | (10) | (11) | (12) | (13) | (14) | (15) |
|------|-------|-------|-------|-------|-------|------|--------|--------|--------|-------|-------|-------|-------|-------|-------|
| (27) | 1.61 | 2.92 | 0.37 | 2.21 | 0.54 | 0.05 | 7.05 | 8.49 | 5.51 | 1.06 | 0.00 | 0.06 | 1.80 | 7.60 | 5.36 |
| (28) | 1.32 | 2.83 | 0.60 | 3.80 | 0.36 | 0.02 | 6.38 | 6.67 | 7.33 | 0.79 | 0.00 | 0.03 | 1.79 | 5.20 | 8.08 |
| (29) | 1.02 | 1.97 | 0.38 | 1.86 | 2.13 | 0.08 | 5.19 | 6.11 | 4.58 | 5.52 | 0.04 | 0.38 | 1.67 | 4.69 | 4.19 |
| to | 29.70 | 87.07 | 11.15 | 80.91 | 24.77 | 2.23 | 129.67 | 140.58 | 125.10 | 51.91 | 23.06 | 10.49 | 65.51 | 88.31 | 86.72 |
| (16) | (17) | (18) | (19) | (20) | (21) | (22) | (23) | (24) | (25) | (26) | (27) | (28) | (29) | from | |
| (1) | 0.10 | 2.21 | 1.88 | 0.34 | 0.00 | 0.12 | 0.03 | 0.02 | 0.13 | 0.24 | 1.24 | 3.69 | 3.08 | 0.31 | 46.38 |
| (2) | 0.13 | 5.08 | 4.54 | 0.35 | 0.05 | 0.17 | 0.04 | 0.00 | 0.10 | 0.19 | 1.11 | 3.75 | 3.67 | 0.32 | 70.09 |
| (3) | 0.00 | 0.79 | 1.02 | 0.56 | 0.08 | 0.21 | 0.08 | 0.08 | 0.13 | 0.00 | 0.41 | 1.19 | 1.94 | 0.55 | 24.93 |
| (4) | 0.10 | 4.11 | 5.94 | 0.41 | 0.12 | 0.19 | 0.13 | 0.01 | 0.18 | 0.08 | 0.85 | 2.90 | 5.05 | 0.41 | 69.38 |
| (5) | 1.96 | 3.58 | 3.19 | 2.64 | 0.13 | 0.33 | 0.11 | 0.003 | 0.60 | 1.10 | 1.33 | 2.72 | 2.43 | 4.37 | 65.92 |
| (6) | 0.45 | 0.02 | 0.07 | 0.05 | 0.14 | 0.23 | 0.14 | 0.18 | 0.67 | 0.15 | 0.13 | 0.33 | 0.16 | 0.36 | 5.55 |
| (7) | 0.33 | 6.20 | 5.52 | 0.50 | 0.06 | 0.28 | 0.20 | 0.02 | 0.20 | 0.27 | 1.78 | 6.18 | 5.65 | 0.86 | 79.58 |
| (8) | 0.64 | 6.50 | 5.28 | 0.57 | 0.07 | 0.31 | 0.14 | 0.00 | 0.29 | 0.28 | 1.99 | 7.08 | 5.62 | 1.26 | 80.61 |
| (9) | 0.52 | 5.63 | 6.74 | 0.56 | 0.12 | 0.29 | 0.22 | 0.003 | 0.23 | 0.21 | 1.53 | 4.91 | 6.59 | 0.80 | 79.27 |
| (10) | 2.28 | 4.68 | 4.16 | 3.81 | 0.19 | 0.36 | 0.15 | 0.03 | 1.21 | 0.89 | 1.71 | 4.79 | 4.23 | 5.00 | 85.68 |
| (11) | 0.12 | 0.04 | 0.04 | 0.01 | 18.51 | 0.89 | 0.38 | 0.08 | 3.09 | 1.81 | 0.09 | 0.08 | 0.06 | 0.21 | 27.63 |
| (12) | 0.44 | 1.70 | 1.50 | 0.70 | 0.55 | 0.99 | 1.10 | 0.00 | 4.09 | 1.70 | 0.77 | 1.43 | 1.35 | 1.67 | 40.66 |
| (13) | 0.95 | 3.31 | 2.92 | 0.90 | 0.51 | 2.87 | 2.55 | 0.11 | 4.58 | 3.91 | 1.64 | 3.55 | 3.50 | 1.20 | 59.42 |
| (14) | 1.36 | 4.05 | 2.54 | 0.18 | 0.18 | 0.16 | 0.10 | 0.02 | 0.25 | 0.24 | 1.54 | 9.23 | 6.37 | 0.97 | 71.80 |
| (15) | 1.27 | 3.32 | 4.19 | 0.23 | 0.13 | 0.09 | 0.10 | 0.08 | 0.17 | 0.19 | 0.97 | 6.46 | 9.80 | 0.78 | 72.05 |
| (16) | 26.61 | 2.66 | 2.27 | 1.89 | 0.12 | 0.17 | 0.06 | 0.04 | 1.20 | 0.44 | 0.80 | 6.75 | 5.90 | 8.30 | 73.39 |
| (17) | 0.38 | 23.75 | 19.49 | 1.42 | 0.01 | 0.54 | 0.30 | 0.01 | 0.11 | 0.32 | 2.32 | 5.77 | 4.93 | 0.66 | 76.25 |
| (18) | 0.39 | 20.00 | 24.37 | 1.47 | 0.00 | 0.44 | 0.30 | 0.02 | 0.10 | 0.18 | 1.68 | 4.37 | 6.15 | 0.58 | 75.63 |
| (19) | 1.55 | 14.98 | 13.73 | 20.30 | 0.01 | 0.51 | 0.28 | 0.01 | 0.42 | 0.31 | 1.87 | 3.62 | 3.57 | 3.25 | 79.70 |
| (20) | 0.07 | 0.16 | 0.13 | 0.03 | 68.51 | 0.17 | 0.13 | 0.03 | 3.12 | 1.48 | 0.11 | 0.89 | 0.64 | 1.12 | 31.49 |

(Continues)

TABLE A1 (Continued)

| | (16) | (17) | (18) | (19) | (20) | (21) | (22) | (23) | (24) | (25) | (26) | (27) | (28) | (29) | from |
|------|-------|--------|--------|-------|-------|-------|-------|-------|-------|-------|-------|--------|--------|-------|-------|
| (21) | 0.15 | 1.45 | 1.16 | 0.59 | 0.17 | 60.90 | 16.90 | 0.11 | 1.87 | 1.77 | 0.47 | 1.18 | 1.37 | 0.49 | 39.10 |
| (22) | 0.02 | 0.95 | 0.95 | 0.32 | 0.12 | 18.10 | 66.17 | 0.69 | 1.39 | 1.05 | 0.34 | 0.45 | 0.83 | 0.14 | 33.83 |
| (23) | 0.14 | 0.02 | 0.07 | 0.01 | 0.04 | 0.18 | 1.01 | 97.08 | 0.05 | 0.05 | 0.01 | 0.02 | 0.01 | 0.04 | 2.92 |
| (24) | 1.88 | 2.75 | 2.32 | 1.00 | 1.91 | 1.54 | 1.19 | 0.03 | 41.19 | 6.96 | 0.94 | 2.26 | 2.10 | 3.81 | 58.81 |
| (25) | 0.76 | 1.53 | 1.12 | 0.46 | 1.15 | 1.68 | 1.00 | 0.03 | 8.86 | 53.94 | 0.46 | 1.26 | 1.03 | 1.52 | 46.06 |
| (26) | 0.19 | 5.07 | 3.62 | 1.41 | 0.05 | 0.38 | 0.25 | 0.00 | 0.48 | 0.18 | 52.50 | 3.45 | 2.23 | 1.11 | 47.50 |
| (27) | 0.69 | 5.69 | 4.20 | 0.24 | 0.23 | 0.44 | 0.15 | 0.00 | 0.19 | 0.20 | 1.53 | 23.20 | 16.52 | 2.09 | 76.80 |
| (28) | 0.63 | 4.78 | 5.81 | 0.30 | 0.13 | 0.50 | 0.28 | 0.003 | 0.23 | 0.11 | 0.98 | 16.35 | 22.97 | 1.72 | 77.03 |
| (29) | 4.68 | 3.82 | 3.32 | 2.33 | 0.36 | 0.40 | 0.15 | 0.01 | 1.40 | 0.48 | 1.17 | 13.89 | 12.22 | 15.98 | 84.02 |
| to | 22.17 | 115.07 | 107.71 | 23.27 | 25.15 | 32.53 | 27.47 | 1.62 | 35.32 | 24.77 | 29.76 | 118.55 | 117.01 | 43.90 | 57.98 |

Note: The main body of this connectedness tables shows the net pairwise directional spillovers between the different futures markets. The right-most column and the bottom row summarize the total directional spillovers *from* and *to* other markets.